BAMBI - A Transient Two-Dimensional Device Simulator Using Implicit Backward Euler's Method and a Totally Self Adaptive Grid

W.KAUSEL, G.NANZ, S.SELBERHERR, H.PÖTZL

Institut für Allgemeine Elektrotechnik und Elektronik
Dept. for CAE
Technical University of Vienna
Gußhausstraße 27-29, A-1040 Vienna, AUSTRIA

Abstract - We present a two-dimensional transient simulator applicable to any given structure (bipolar or MOS, HF- or power device) based on a totally self-consistent solution of the three basic semiconductor equations. Fully self-adaptive control is given for both space and time discretization.

Furthermore we present a complete simulation of the turn off behavior of a realistic short channel MOS-transistor ($L_{eff} = 0.68\mu m$). The transistor is switched from a bias point in the ohmic part of the characteristic into the off state. The transient response of all interesting quantities (i.e. electron and hole concentrations, potential and field, electron and hole current densities) is documented.

BAMBI - A Transient Two-Dimensional Device Simulator Using Implicit Backward Euler's Method and a Totally Self Adaptive Grid

W.KAUSEL, G.NANZ, S.SELBERHERR, H.PÖTZL

Institut für Allgemeine Elektrotechnik und Elektronik
Dept. for CAE
Technical University of Vienna
Gußhausstraße 27-29, A-1040 Vienna, AUSTRIA

The transient behavior of bipolar and MOS devices is of great interest for many semiconductor designers and technologists. We present essential improvements in time and space discretization implemented in the two-dimensional transient simulator BAMBI which is applicable to any given structure (bipolar or MOS, HF- or power device). The analysis is based on a totally self-consistent solution of the three basic semiconductor equations. A fully self-adaptive first order Finite Boxes grid is used for space discretization The implicit backward Euler's method, which is absolutely stable for any stepwidth, is adapted for time discretization.

The accuracy of the space discretization is controlled by the widely used analysis of the local discretization error of Poisson's equation. Since the equidistribution of the local discretization error does not always provide an optimal space grid, two additional criteria for grid design have been tested: (1) geometrical information about singularities in the solution of the electrostatic potential (for the initial grid) and (2) the magnitude of the Bernoulli function.

The design of an initial space grid is usually based on an analysis of the doping profile. This fails, if a constant doping is assumed (e.g. MESFET's). By introducing new grid points near singularities of the electric field (change from contact to Neumann boundary, origin of a cylindrically symmetric coordinate system) difficulties for initial meshes which do not account for singular points can be avoided.

Assuming a finite differences discretization of the three basic semiconductor equations the coupling of the equations is mainly determined by the Bernoulli function $B(x) = \frac{x}{e^x - 1}$, where x denotes the difference of the electrostatic potential at two neighbouring grid points divided by the thermal voltage. A local decoupling of the equations because of vanishing values of B may cause numerical difficulties. Especially at contact points (elliptic problem) a decoupling may lead to a singular system.

For the estimation of the time discretization error the change in space charge density from one time step to the following is analyzed.

$\Delta\rho = \|\rho_{t+1} - \rho_t\| = \|p_{t+1} - p_t - (n_{t+1} - n_t)\|$

If ρ changes by more than 10% the last time step is decreased and computed again. The space discretization criteria are checked every third time step. If the criterion is not fulfilled, new points are inserted. For the interpolation of the solution at the inserted points the last time step is computed again with the old points treated as Dirichlet points. The computational error introduced by this interpolation is reduced by two quasi-zero time steps which enable

the relaxation of the space charge. The contact currents are very sensitive to any change in the solution as it can be seen in (Fig. 1). These two very small time steps cause completely wrong and even oscillating results which can be suppressed in the output, but in the third step a correct value of the current is gained (Fig. 2). Two intermediate steps are sufficient because of the first order discretization.

In addition we prove the capability of the model with a transient simulation of the turn off behavior of a realistic short channel NMOS-transistor ($L_{eff} = 0.68\mu m$, $d_{ox} = 250Å$, channel doping at the interface $= 1.10^{17}cm^{-3}$, substrate doping $= 6.10^{15}cm^{-3}$). The transistor is switched from a bias point in the ohmic part of the characteristic ($V_{ds} = 5V$, $V_{gs} = 7V$, $V_{sb} = 0V$) into the off state ($V_{ds} = 5V$, $V_{gs} = -0.3V$, $V_{sb} = 0V$). The transient response of all interesting quantities (i.e.: electron and hole concentrations, potential and field, electron and hole current densities) is post-processed and analyzed by quasi three-dimensional plots. The simulation shows that the potential in the channel region jumps due to the capacitive effect of the gate voltage pulse from positive to negative values causing a high increase in the electric field on source and on drain side of the channel region (Fig. 3,4). Consequently the channel electrons flow out of the channel at both sides to drain and to source. As our analysis proves a non-negligible diffusion of electrons into the bulk region occurs. Finally the figure of the contact currents shows that the capacitive displacement current is dominating within the first 2ps leading to higher values for the source current whereas lateral field current dominates after 2ps with higher values for drain current.

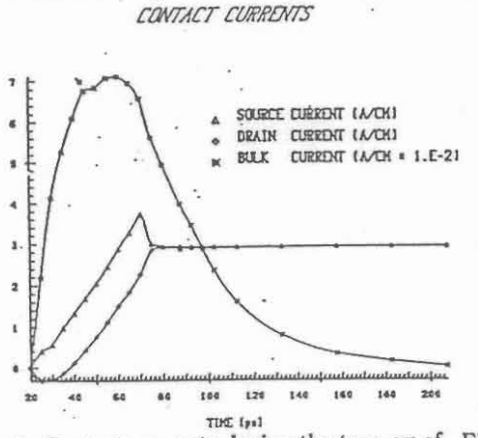

Fig.1: Contact currents during the turn on of a NMOS-transistor without correction

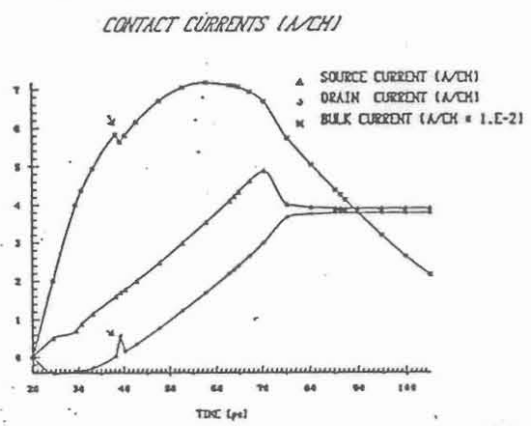

Fig.2: Contact currents during the turn on of a NMOS-transistor with two intermediate time steps

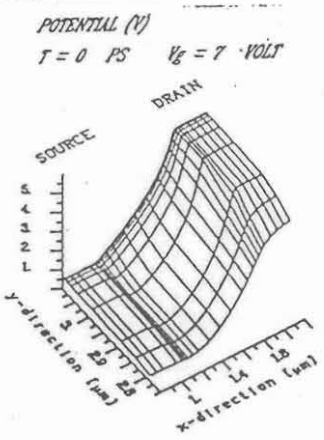

Fig.3: Steady state potential distribution in the channel region before the gate voltage pulse

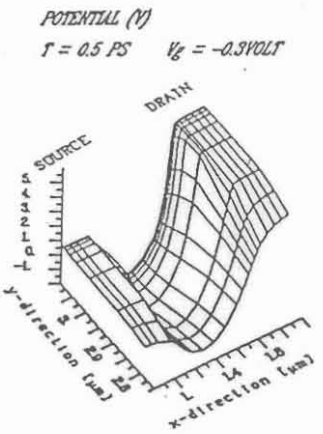

Fig.4: Potential distribution in the channel region immediatly after the gate voltage pulse